

## SIMULATION OF CAPACITIVELY COUPLED RF DISCHARGE IN ARGON

V. Lisovskiy, S. Dudin, A. Shakhnazarian, P. Platonov, V. Yegorenkov  
V.N. Karazin Kharkiv National University, Kharkiv, Ukraine  
E-mail: lisovskiy@yahoo.com

In this work, the axial profiles of the density of electrons and positive ions, the mean electron energy, the electric field strength, and the potential were obtained, both on average over the period and in dynamics. It was shown that argon discharges are dominated by ionization by electrons that gained energy by stochastic heating during the expansion of near-electrode sheaths. This ionization occurs in two pulses during one RF period. At low RF voltage between the electrodes, the role of Ohmic heating of electrons in the electric field in a quasi-neutral plasma increases, but the contribution of stochastic heating remains dominant. The time-averaged plasma potential was found to increase non-linearly with the RF voltage between the electrodes  $U_{rf}$ . It is shown that at low  $U_{rf}$  values (when the RF voltage approaches the discharge extinction curve), the average potential  $\Phi$  can reach  $U_{rf}$  due to the axial redistribution of the instantaneous potential in the gap between the electrodes.

PACS: 52.80.Hc

### INTRODUCTION

Radio-frequency capacitive discharge in gases is widely used in many plasma technologies. With its help, various materials are sputtered, various films are deposited (both metal and dielectric), semiconductor materials are etched during the production of microchips, gas discharge lasers are pumped, and the surfaces of technological and research chambers are cleaned (from centimeter size to the scale of large tokamaks and stellarators), etc. Therefore, considerable attention is paid to both experimental and theoretical research of its properties. Usually, either the external parameters of the RF capacitive discharge (for example, the current-voltage characteristics) or the time-averaged plasma parameters are measured experimentally [1 - 7]. But in order to understand exactly how the processes of birth and loss of charged particles take place, and what the dynamics of the internal parameters of the plasma look like, numerical modeling is frequently used [2, 7 - 9].

The purpose of this work was to carry out numerical modeling of the parameters of a radio-frequency capacitive discharge in argon using the SIGLO-rf hydrodynamic code. Plasma parameters averaged over the RF period were determined, and their changes with time were investigated. The mechanisms of ionization, the time and place within the discharge, where and when they occur, have been clarified.

### 1. DESCRIPTION OF SIGLO-RF CODE

SIGLO-rf is fluid code, which is the 1D user-friendly simulation software of capacitively coupled RF discharges. It was developed by JP Boeuf and LC Pitchford at the University of Toulouse and is based on the same physics as in [10, 11].

SIGLO-rf numerically solves the continuity, momentum, and energy equations for electrons, the discontinuity and momentum equations for positive ions, and Poisson's equation for the electric field.

In the axial profiles shown in the next section, the left electrode is grounded, and RF voltage  $U_{rf}$  oscillating with a frequency of 13.56 MHz is applied to the right electrode. The distance between the electrodes is fixed and is 2 cm. The gas pressure is 1 Torr.

Calculations were made for argon. Accordingly, the necessary information was entered into the file with gas parameters. The dependences of electron mobility, average electron energy, and ionization coefficient (the first Townsend coefficient  $\alpha/p$ ) on the reduced electric field  $E/p$  for gas temperature  $T = 300$  K were preliminarily calculated using the Bolsig+ code [12]. At the same time, cross-sections of electron collisions with argon atoms were used, given in the LXCat database ([www.lxcat.net](http://www.lxcat.net)) [13], where cross-sections from the Phelps set [14] were selected.

In addition, for argon, the mobilities of positive Ar<sup>+</sup> ions in Ar, given in the review [15], were used. Ion-electron recombination was neglected due to the very small value of the coefficient for this process [16].

### 2. EXPERIMENTAL RESULTS

RF capacitive discharge consists of three regions, a quasi-neutral plasma and two sheaths of space charge, which are actually transition parts between the plasma and the electrode walls limiting it. Quasi-neutral plasma and near-electrode sheaths differ greatly in terms of parameters. At the same time, it is necessary to consider not only the average parameters of the discharge over the RF period but also to take into account that these parameters also change over time due to the harmonic change of the RF voltage on the right (potential) electrode. Therefore, below we will present the average profiles of plasma parameters for the RF period, and for some of them, we will find out their dynamics.

The time-averaged axial profiles of electron density  $N_e$  and positive ion density  $N_p$  are shown in Fig. 1. It can be seen from the figure that the quasi-neutrality condition is fulfilled in the plasma volume, that is, the densities of electrons and positive ions are equal to each other, and the corresponding parts of the curves in the figure coincide.

The near-electrode sheaths are dominated by positive ions, and the electron density here is much lower than the ion density. That is, here we observe a violation of the condition of quasi-neutrality. From the plasma to the boundary of the sheaths, positive ions and electrons move in the mode of ambipolar diffusion, so their densities in the plasma are the same.

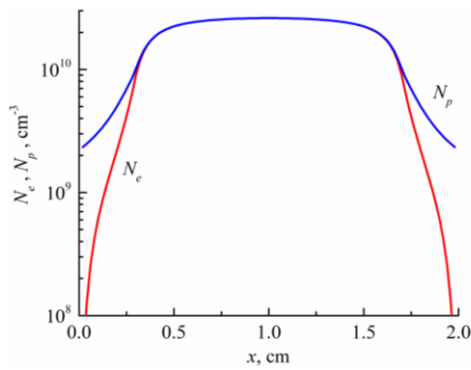


Fig. 1. Time-averaged axial profiles of the density of electrons and positive ions

But after reaching the limit of the plasma region, positive ions are accelerated to the electrodes by a strong electric field averaged over time, the voltage of which increases approximately according to a linear law when approaching the electrodes (Fig. 2). In a quasi-neutral plasma, this field is small (approximately units V/cm and increases to 20 V/cm at the boundary of the sheaths) but it is zero only in the center of the discharge gap. In the considered case, the average electric field strength near the electrode surface approaches 1400 V/cm.

As a result of the oscillations of the electrons in the instantaneous radio-frequency electric field, some of them enter the electrodes. Therefore, there are more positive ions than electrons in the discharge gap. Thanks to this, the plasma has a positive potential in relation to the electrodes. Let us recall that the left electrode is grounded, and the potential of the right electrode changes according to the harmonic law and is also zero on average during the RF period. Therefore, positive ions are accelerated by this electric field averaged over the RF period from the plasma to the electrodes, due to which the RF capacitive discharge has found wide application in many plasma technologies.

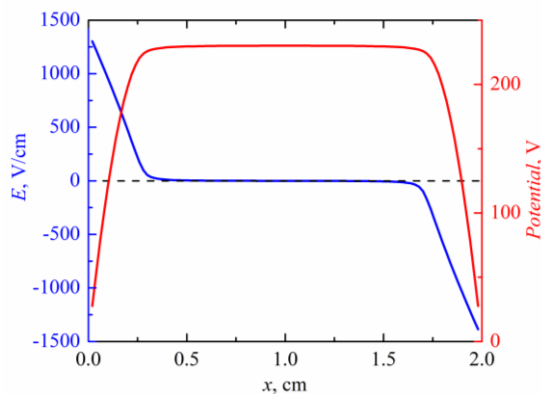


Fig. 2. Time-averaged axial profiles of potential and electric field strength

The value of the average plasma potential depends on the RF voltage applied to the electrodes, the pressure, and the type of gas. For argon gas at 1 Torr pressure and 500 V RF voltage, the average plasma potential (for the center of the discharge) is about 230 V (see Fig. 2).

Now let's consider the time-averaged axial profiles of the mean electron energy, which are shown in Fig. 3. From the figure, one can see that the mean electron energy in the plasma reaches up to approximately 6 eV,

however, in the space charge sheaths, it quickly decreases down to 1 eV near the electrodes. But here, it should be taken into account that electrons alternately fill the near-electrode sheaths, and during certain parts of the RF period they are not present near the electrodes at all, and, accordingly, their average energy is considered zero in this case.

Fig. 3 also shows the time-averaged axial profile of the ionization rate. From its unit of measurement,  $\text{cm}^{-3}\cdot\text{s}^{-1}$ , it is clear that this value is equal to the product of the electron density and the ionization frequency  $\nu_i N_e$  and is the term of the electron and ion balance equation, which describes the rate of ionization birth of charged particles in  $1 \text{ cm}^3$  per 1 s at a certain point in the discharge gap. The maximum values of the ionization rate appear near the boundaries of the near-electrode sheaths and indicate the presence of enhanced electron heating in these areas. A much lower ionization rate is observed in the central part of the discharge gap. We will consider the processes of electron heating below.

Now let's pay attention to the time dependences of the axial profiles of the plasma parameters. First, let's consider the profiles of the plasma potential for several moments of time during one-half of the RF period (Fig. 4). At the initial moment, when the high-amplitude RF voltage is applied to the right electrode, almost the entire potential drop is concentrated on the left near-electrode sheaths, because the left electrode plays the role of an instantaneous cathode. In the left sheaths, the electric field strength is maximum, and the right sheaths has practically collapsed. A flow of electrons enters the right electrode, which is limited by a small voltage drop near the electrode.

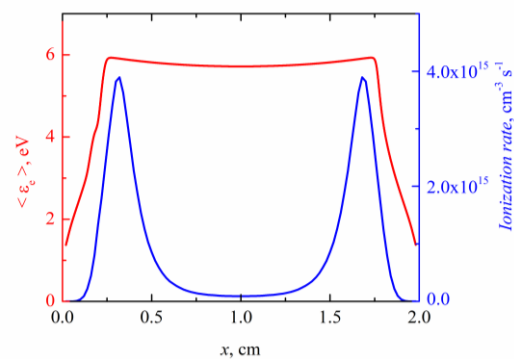


Fig. 3. Time-averaged axial profiles of average electron energy and ionization rate

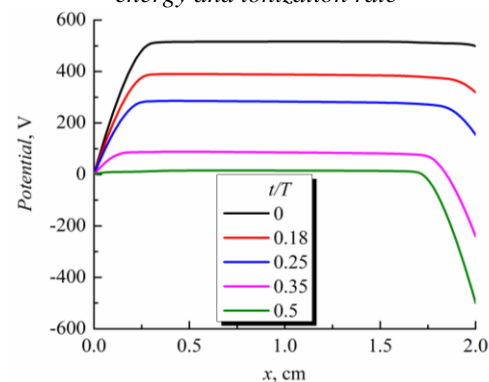


Fig. 4. Axial profiles of potential for different parts of RF period for voltage between the electrodes of 500 V

Then, over time, the voltage drop on the left sheaths decreases with the simultaneous narrowing of the thickness of the left sheaths. At the right electrode, the voltage decreases first to zero, and then further to a negative amplitude value. Throughout this half-period, the thickness of the right sheaths increases. This half-period ends with the reverse situation in relation to the initially considered zero time moment, namely, the left near-electrode sheaths has collapsed, and the left electrode receives a flow of electrons (which is regulated by a small voltage drop near its surface).

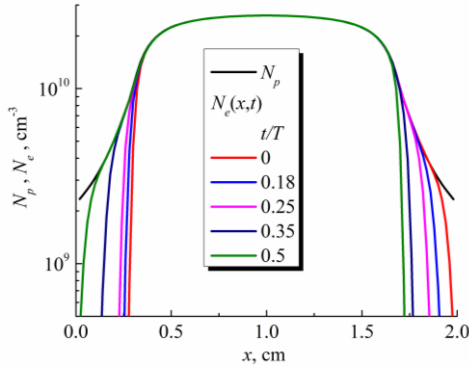


Fig. 5. Axial density profiles of positive ions and electrons for different parts of the period for RF voltage between electrodes of 500 V

The dynamics of the electron density profile for the same moments of time are shown in Fig. 5. The positive ion density profile practically does not change with time, because the frequency of the RF field of 13.56 MHz applied to the electrodes is too high for them. Ions are heavy inert particles, in a discharge they react only to constant (or time-averaged) and low-frequency (less than 1 MHz) electric fields. Light electrons, in the presence of sufficiently frequent collisions with gas molecules, are able to sense changes in the electric field almost without inertia. At the initial moment ( $t/T = 0$ ), electrons are pushed out of the left near-electrode sheaths and, having filled the right sheaths, enter the right electrode (instantaneous anode). At the same time, we note that the electron density profile in the right sheaths practically coincides with the profile of the density of positive ions, with the exception of a narrow region near the very surface of the right electrode. That is, it can be said that quasi-neutral plasma almost completely fills the right sheaths at the initial moment of time. Later, as shown in Fig. 4, the voltage on the right electrode decreases. The plasma potential also decreases, but more slowly than the voltage on the right electrode, so the voltage drop on the right sheaths increases. This leads to the fact that the thickness of the right sheaths increases. Electrons, which initially almost completely filled the right sheaths, are now pushed from the right electrode back into the plasma because the potential of this electrode is now more negative in relation to the plasma. This ejection increases the electron energy and is called stochastic heating [17 - 20]. This stochastic heating led to an increase in the ionization rate near the boundaries of the near-electrode sheaths on the time-averaged axial profiles (see Fig. 3).

Fig. 6 shows in which places and when exactly stochastic heating occurs in the RF capacitive discharge.

The first peak of the ionization rate (it is located on the right in the figure) occurs when electrons are pushed out of the right near-electrode sheaths. The stochastic heating itself affects the ionization rate both in the right sheaths and outside it in the region of quasi-neutral plasma near the sheaths boundary. At the same time, electrons fill the left sheaths. After the potential on the right electrode reaches the maximum negative value, the voltage on the left sheaths begins to increase. This increase in voltage pushes electrons out of the left sheaths, and as a result of stochastic heating, we observe a spike in the ionization rate, which is on the left in Fig. 6.

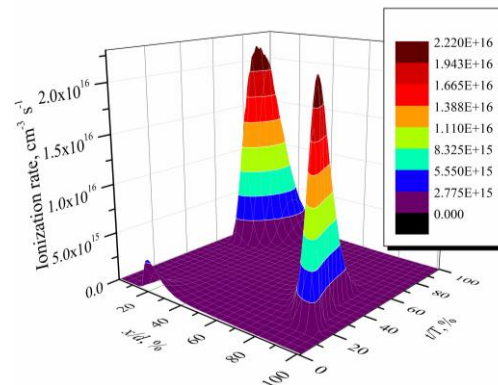


Fig. 6. Spatio-temporal dependence of ionization rate for RF voltage between electrodes of 500 V

Let's note one more important feature of RF capacitive discharge, which occurs in any gas, namely, the balance of positive and negative charges arriving on the surface of each of the electrodes. Fig. 7 shows the current densities of positive ions and electrons that reach the surface of the left electrode during one RF period. It can be seen from the figure that the flow of positive ions is maximal at the beginning and at the end of the RF period (corresponding to the amplitude of positive RF voltage on the right electrode).

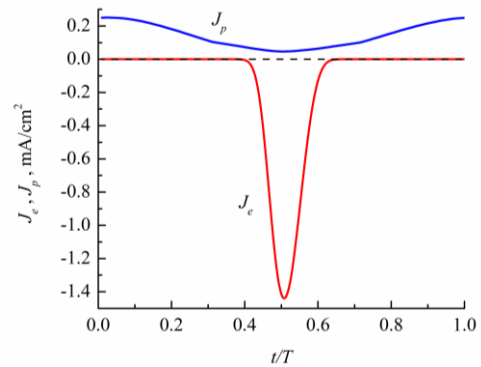


Fig. 7. Time dependence of the current density of positive ions and electrons on the left electrode for RF voltage between the electrodes of 500 V

In the middle of the period, the ion flow decreases, but not to zero. That is, during the entire RF period, positive ions arrive on the surface of the left electrode. Electrons also arrive at the same electrode but in the form of a short burst with a maximum when the RF voltage on the right electrode reaches the negative amplitude value. Therefore, for the stable burning of the discharge, it is necessary that the balance of positive and negative charges be fulfilled, that is, the number of electrons that entered the left electrode during the burst

shown in the figure was equal to the number of positive ions that reached the surface of this electrode during the entire RF period. The areas under the  $J_p$  and  $J_e$  curves (between these curves and the abscissa axis) must be equal to each other.

Above we presented the results for a fixed value of the RF voltage  $U_{rf} = 500$  V applied to the electrodes. Below, we will consider the dependence of the plasma parameters on  $U_{rf}$ , in the range from the discharge extinction voltage (the minimum voltage at which the RF discharge is possible to burn, for 1 Torr it is equal to 27 V) to 1000 V. The RF voltage decrease leads to increase in RF electric field strength in the plasma (Fig. 8) with a simultaneous decrease in the rate of ionization due to stochastic heating. This leads to an increase in the role of Ohmic heating of electrons in the plasma, the contribution of which to the ionization rate can reach a third of the contribution of stochastic heating at low RF voltages (Fig. 9).

Note the interesting behavior of the time-averaged plasma potential (this is the potential of the center of the discharge relative to the electrodes, averaged over the RF period), which we denote as  $\Phi$  (Fig. 10). This potential increases monotonically with increasing RF voltage on the electrodes. Analytical theory [19] assumes that  $\Phi = (3/8) U_{rf}$ . But calculations using the SIGLO-rf code show that this dependence is not linear. Moreover, as the  $U_{rf}$  voltage decreases, the ratio  $U_{rf}/\Phi$  also decreases, and at low RF voltages, especially before the discharge extinction, the average plasma potential  $\Phi$  may even slightly exceed the amplitude of the RF voltage on the electrodes  $U_{rf}$  (see Fig. 10).

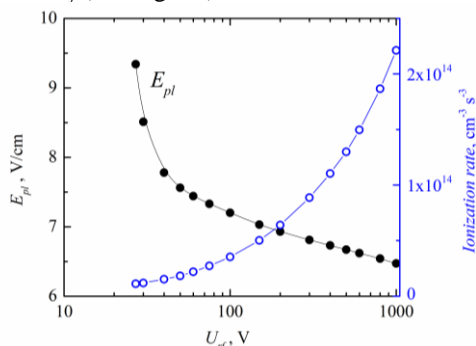


Fig. 8. Dependence of the amplitude of the RF electric field in the center of the plasma and the maximum values of the ionization rate on the RF voltage applied to the electrodes

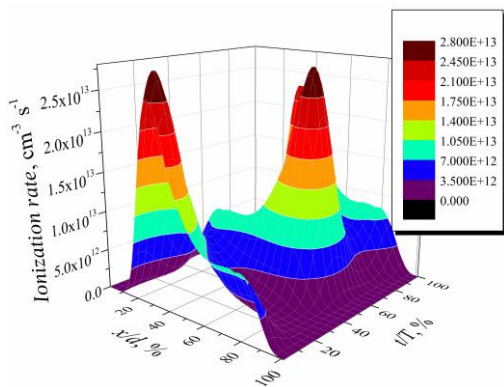


Fig. 9. Spatio-temporal dependence of the ionization rate for the RF voltage between the electrodes of 27 V

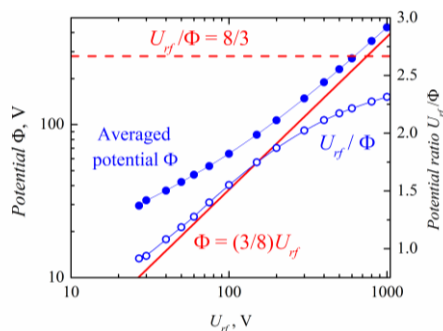


Fig. 10. Dependence of the time-averaged potential  $\Phi$  in the center of the plasma on the amplitude of the RF voltage between the electrodes  $U_{rf}$ , as well as the ratio  $U_{rf}/\Phi$  on  $U_{rf}$

This is explained by the redistribution of the potential between the electrodes under conditions of low the density of charged particles in the plasma, which is shown in Fig. 11 for different moments of the RF period. We see that the potential of the middle of the discharge varies from 17 V ( $t/T = 0.5$ ) to 43 V ( $t/T = 0$ ) at different times, that is, the plasma always has a positive instantaneous potential relative to the grounded electrode. It should be noted that even at a high RF voltage of 500 V (see Fig. 4), the plasma relative to the electrode (momentary anode) had a potential of approximately 15 V, which corresponds to the magnitude of the anode voltage drop of the DC discharge [21].

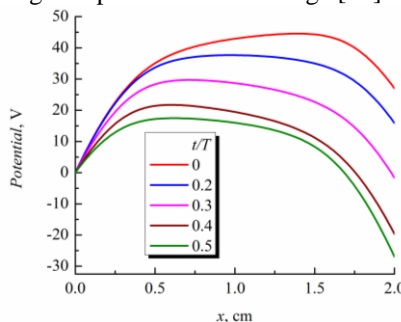


Fig. 11. Axial potential profiles for different parts of the period for RF voltage between electrodes of 27 V

## CONCLUSIONS

In the present research, the structure and properties of a radio-frequency capacitive discharge in argon are investigated using the one-dimensional hydrodynamic code SIGLO-rf. As a result of calculations, this code allows obtaining axial profiles of charged particles (electrons, ions), the average energy of electrons, potential, and electric field strength both at specific moments of the RF period and on average over the period. Additionally, the current density of each type of charged particle is determined both on the electrodes and in the plasma volume.

The dynamics of the density of charged particles, the potential and the rate of ionization in the RF capacitive discharge were also studied. It was shown that the most intense ionization in a discharge in argon occurs in two pulses during one RF period due to the stochastic heating of electrons. Electrons that during the anode phase filled, for example, the right near-electrode sheath, during the next expansion of this sheath are pushed into the plasma and acquire energy that allows them to ionize

argon atoms. After half of the RF period, stochastic heating repeats in the opposite near-electrode sheath during its expansion.

It is shown that the time-averaged plasma potential  $\Phi$  depends nonlinearly on the RF voltage between the electrodes  $U_{rf}$ , and at low  $U_{rf}$  values this potential can reach (and even slightly exceed)  $U_{rf}$ . This is observed when the RF voltage approaches the discharge extinction curve and is explained by the redistribution of voltage between the electrodes, thanks to which the quasi-neutral plasma of the RF capacitive discharge is positive relative to even the instantaneous anode.

#### ACKNOWLEDGEMENT

This work was supported by the National Research Foundation of Ukraine in the framework of the project 2021.01/0204.

#### REFERENCES

1. V.A. Godyak, R.B. Piejak, B. Alexandrovich. Electrical characteristics of parallel-plate RF discharges in argon // *IEEE Trans. Plasma Sci.* 1991, v. 19, p. 660-676.
2. D.A. Schulenberg, I. Korolov, Z. Donkó, A. Derzsi, J. Schulze. Multi-diagnostic experimental validation of 1d3v PIC/MCC simulations of low pressure capacitive RF plasmas operated in argon // *Plasma Sources Sci. Technol.* 2021, v. 30, p. 105003 (13 p).
3. V.A. Lisovskiy. Features of the  $\alpha$ - $\gamma$  Transition in a low-pressure rf argon discharge // *Technical Physics*. 1998, v. 43, p. 526-534.
4. V. Lisovskiy, J.-P. Booth, K. Landry, V. Cassagne, V. Yegorenkov. Modes and the alpha-gamma transition in rf capacitive discharges in  $N_2O$  at different rf frequencies // *Physics of Plasmas*. 2006, v. 13, p. 103505.
5. V. Lisovskiy, J.-P. Booth, J. Jolly, V. Cassagne, V. Yegorenkov. Modes of rf capacitive discharge in low-pressure sulfur hexafluoride // *J. Phys. D: Appl. Phys.* 2007, v. 40, p. 6989-6999.
6. V. Lisovskiy, J.-P. Booth, K. Landry, D. Douai, V. Cassagne, V. Yegorenkov. Rf discharge dissociative mode in  $NF_3$  and  $SiH_4$  // *J. Phys. D: Appl. Phys.* 2007, v. 40, p. 6631-6640.
7. Z. Donkó, J. Schulze, U. Czarnetzki, A. Derzsi, P. Hartmann, I. Korolov, E. Schungel. Fundamental investigations of capacitive radio frequency plasmas: simulations and experiments // *Plasma Phys. Control. Fusion*. 2012, v. 54, p. 124003 (15 p).
8. J. Schulze, E. Schüngel, A. Derzsi, I. Korolov, Th. Mussenbrock, Z. Donkó. Complex electron heating in capacitive multi-frequency plasmas // *IEEE Trans. Plasma Sci.* 2014, v. 42, p. 2780-2781.
9. D.-Q. Wen, J. Krek, J.T. Gudmundsson, E. Kawamura, M.A. Lieberman, P. Zhang, J.P. Verboncoeur. On the importance of excited state species in low pressure capacitively coupled plasma argon discharges // *Plasma Sources Sci. Technol.* 2023, v. 32, p. 064001 (13 p).
10. J.P. Boeuf, L.C. Pitchford. Two-dimensional model of a capacitively coupled rf discharge and comparisons with experiments in the Gaseous Electronics Conference reference reactor // *Phys. Rev. E*. 1995, v. 51, p. 1376-1390.
11. J.P. Boeuf. Numerical model of rf glow discharges // *Phys. Rev. A*. 1987, v. 36, p. 2782-2792.
12. G.J.M. Hagelaar, L.C. Pitchford. Solving the Boltzmann equation to obtain electron transport coefficients and rate coefficients for fluid models // *Plasma Sources Sci. Technol.* 2005, v. 14, p. 722-733.
13. L.C. Pitchford, L.L. Alves, K. Bartschat, S.F. Biagi, M.C. Bordage, et al. LXCat: An Open-Access, Web-Based Platform for Data Needed for Modeling Low Temperature Plasmas // *Plasma Process. Polym.* 2017, v. 14, p. 1600098.
14. C. Yamabe, S.J. Buckman, A.V. Phelps. Measurement of free-free emission from low-energy-electron collisions with Ar // *Phys. Rev. A*. 1983, v. 27, p. 1345-1352.
15. H.W. Ellis, R.Y. Pai, E.W. McDaniel, E.A. Mason, L.A. Viehland. Transport properties of gaseous ions over a wide energy range // *Atomic Data and Nuclear Data Tables*. 1976, v. 17, issue 3, p. 177-210.
16. Yu.P. Raizer. *Gas discharge physics*. Berlin: "Springer", 1991.
17. M.A. Lieberman. Dynamics of a collisional, capacitive RF sheath // *IEEE Trans. Plasma Sci.* 1989, v. 17, p. 338-341.
18. M.A. Lieberman. Analytical solution for capacitive RF sheath // *IEEE Trans. Plasma Sci.* 1988, v. 16, p. 638-644.
19. M.A. Lieberman, A.J. Lichtenberg. *Principles of plasma discharges and materials processing*. New York: "Wiley", 2005.
20. P. Chabert, N. Braithwaite. *Physics of Radio-Frequency Plasmas*. Cambridge: Cambridge University Press, 2011.
21. V.A. Lisovskiy, S.D. Yakovin. Experimental Study of a Low-Pressure Glow Discharge in Air in Large-Diameter Discharge Tubes // *Plasma Physics Reports*. 2000, v. 26, p. 1066-1075.

Article received 15.06.2023

#### МОДЕЛЮВАННЯ ВЧ ЄМНІСНОГО РОЗРЯДУ В АРГОНІ

*В. Лісовський, С. Дудін, А. Шахназарян, П. Платонов, В. Єгоренков*

Отримано осьові профілі густини електронів та позитивних іонів, середньої енергії електронів, напруженості електричного поля та потенціалу як у середньому за період, так й їхню динаміку. Показано, що в розряді в аргоні переважає іонізація електронами, які набули енергії під час стохастичного нагріву при розширенні приелектродних шарів. Ця іонізація відбувається двома імпульсами протягом одного ВЧ-періоду. При низькій ВЧ-напрузі між електродами зростає роль омичного нагріву електронів у електричному полі в квазі-нейтральній плазмі, але внесок стохастичного нагріву залишається домінуючим. З'ясовано, що середній за часом потенціал плазми  $\Phi$  нелінійно зростає з ВЧ-напругою  $U_{rf}$  між електродами. Показано, що при низьких значеннях  $U_{rf}$  (при наближенні ВЧ-напругою до кривої згасання розряду) середній потенціал  $\Phi$  може досягати  $U_{rf}$  завдяки осьовому перерозподілу миттєвого потенціалу в проміжку між електродами.